HAL
open science

Temperature-Dependent Kinetic Study of the Reactions of Hydrogen Atoms with H2S and C2H4S

Yuri Bedjanian

To cite this version:

Yuri Bedjanian. Temperature-Dependent Kinetic Study of the Reactions of Hydrogen Atoms with H2S and C2H4S. Molecules, 2023, 28 (23), pp.7883. 10.3390/molecules28237883 . hal-04360303

HAL Id: hal-04360303

https://cnrs.hal.science/hal-04360303

Submitted on 21 Dec 2023

HAL is a multi-disciplinary open access archive for the deposit and dissemination of scientific research documents, whether they are published or not. The documents may come from teaching and research institutions in France or abroad, or from public or private research centers.

L'archive ouverte pluridisciplinaire **HAL**, est destinée au dépôt et à la diffusion de documents scientifiques de niveau recherche, publiés ou non, émanant des établissements d'enseignement et de recherche français ou étrangers, des laboratoires publics ou privés.

molecules

MDPI

Article

Temperature-Dependent Kinetic Study of the Reactions of Hydrogen Atoms with H_2S and C_2H_4S

Yuri Bedjanian

Institut de Combustion, Aérothermique, Réactivité et Environnement (ICARE), CNRS, 45071 Orléans, France; yuri.bedjanian@cnrs-orleans.fr; Tel.: +33-23-825-5474

Abstract: A discharge-flow reactor combined with modulated molecular beam mass spectrometry technique was employed to determine the rate constants of H-atom reactions with hydrogen sulfide and thiirane. The rate constants for both reactions were determined at a total pressure of 2 Torr from 220 to 950 K under pseudo-first-order conditions by monitoring either consumption of H atoms in excess of H_2S (C_4H_4S) or the molecular species in excess of atomic hydrogen. For H + H_2S reaction, a suggested previously strong curvature of the Arrhenius plot was confirmed: $k_1 = 8.7 \times 10^{-13} \times (T/298)^{2.87} \times \exp(-125/T)$ cm^3 molecule^{-1} s^{-1} with a conservative uncertainty of 15% at all temperatures. Non-Arrhenius behavior was also observed for the reaction of H-atom with C_2H_4S, with the experimental rate constant data being best fitted to a sum of two exponential functions: $k_2 = 1.85 \times 10^{-10} \exp(-1410/T) + 4.17 \times 10^{-12} \exp(-242/T)$ cm^3 molecule^{-1} s^{-1} with an independent of temperature uncertainty of 15%.

Keywords: hydrogen atom; hydrogen sulfide; thiirane; H_2S; C_2H_4S; kinetics; rate constant

check for updates

Citation: Bedjanian, Y. Temperature-Dependent Kinetic Study of the Reactions of Hydrogen Atoms with H_2S and C_2H_4S. *Molecules* **2023**, *28*, 7883. https://doi.org/10.3390/molecules28237883

Academic Editor: Boris Solomonov

Received: 25 October 2023
Revised: 16 November 2023
Accepted: 29 November 2023
Published: 30 November 2023

Copyright: © 2023 by the author. Licensee MDPI, Basel, Switzerland. This article is an open access article distributed under the terms and conditions of the Creative Commons Attribution (CC BY) license (https://creativecommons.org/licenses/by/4.0/).

1. Introduction

The present work reports temperature-dependent measurements of rate constants for two elementary reactions involving hydrogen atoms, with H_2S and C_2H_4S. The H-atom reaction with H_2S is of importance in combustion chemistry and industrial processes, and is included in a detailed chemical mechanism to describe reactions in the H_2–S_2–H_2S system [1]:

$$H + H_2S \rightarrow SH + H_2 \quad (1)$$

The temperature dependence of the rate constant of reaction (1), which proceeds through the abstraction of a hydrogen atom, is also of theoretical interest, in particular for assessing the effect of quantum tunneling [2,3]. Reaction (1) has been intensively studied over the past few decades, both experimentally [4–15] and theoretically [2,3,13,15,16]. Although there is now some experimental and theoretical evidence for the curvature of the Arrhenius plot for reaction (1), it has never actually been observed experimentally in any single study conducted over a sufficiently wide temperature range. All previous experimental work was carried out over a limited temperature range, and "unmodified" Arrhenius expressions were reported for the reaction rate constant. One of the aims of this work was to provide experimental evidence of the curvature of the Arrhenius dependence of k_1 within the framework of one study through rate constant measurements over an extended temperature range, T = 220–950 K.

It is known that reactions of C_2H_4S (thiirane, ethylene sulfide) with various atoms are rapid and proceed through S-atom abstraction, leading to almost stoichiometric production of ethylene and sulfur-containing radicals [17–20]. This allows the desulfurization reactions of thiirane to be used in laboratory research both as sources of radicals and as scavengers of unwanted active species. The reaction of C_2H_4S with hydrogen atoms leads to the formation of SH (an important intermediate in atmospheric and combustion chemistry [21,22]), and can be used as an alternative source of SH radicals to those involving H_2S [23].

$$H + C_2H_4S \rightarrow SH + C_2H_4 \quad (2)$$

The kinetic information on reaction (2) is rather scarce and uncertain. Only two measurements of the reaction rate constant were reported, by Yokota et al. [24] at T = 300–425 K using the relative rate method, and in absolute measurements by Lee et al. from 223 to 423 K [20]. The activation energies reported in two studies are very close; however, the absolute values of the reaction rate constant differ by a factor of 3. The objective of the present work was to provide new measurements of the rate constant over an extended temperature range, T = 220–950 K.

2. Results and Discussion

2.1. Reaction H + H_2S

2.1.1. Measurements of the Reaction Rate Constant

All measurements were carried out under flow conditions at nearly 2 Torr of total pressure of Helium, and with detection of the gas phase species involved using mass spectrometry [23].

The reaction rate constant was determined under pseudo-first-order conditions either from H_2S decays ($[H_2S]_0 \leq 4 \times 10^{11}$ molecule cm^{-3}) in excess of hydrogen atoms, or from the kinetics of H-atom consumption ($[H]_0 \leq 2 \times 10^{11}$ molecule cm^{-3}) monitored in excess of hydrogen sulfide. The concentrations of the excess reactants were varied between 0.18 and 6.64 × 10^{13} molecule cm^{-3} for H-atom, and between 0.85 and 44.7 × 10^{13} molecule cm^{-3} for $[H_2S]$ (see Table 1). The linear flow velocity in the reactor was in the range of 1025–3400 cm s^{-1}.

Table 1. Experimental conditions and results of the measurements of the rate constant of reaction (1).

T (K)	[Excess Reactant] [a]	k_1 [b]	Reactor Surface [c]	Method [d]
220	6.51–24.2	0.24 ± 0.01	HW	H kinetics
235	4.80–28.8	0.26 ± 0.01	HW	H kinetics
250	3.66–28.4	0.31 ± 0.01	HW	H kinetics
270	1.60–44.7	0.39 ± 0.01	HW	H kinetics
285	0.85–27.8	0.49 ± 0.01	HW	H kinetics
295	0.66–4.37	0.60 ± 0.01	Q	H_2S kinetics
305	1.09–19.7	0.59 ± 0.01	Q	H kinetics
325	1.25–20.4	0.77 ± 0.02	HW	H kinetics
330	0.46–6.64	0.88 ± 0.02	HW	H_2S kinetics
360	0.62–5.58	1.07 ± 0.02	Q	H_2S kinetics
410	0.45–4.60	1.58 ± 0.02	Q	H_2S kinetics
475	0.57–5.87	2.61 ± 0.03	Q	H_2S kinetics
575	0.43–4.46	4.61 ± 0.08	Q	H_2S kinetics
720	0.33–3.31	9.96 ± 0.08	Q	H_2S kinetics
950	0.18–2.61	20.6 ± 0.3	Q	H_2S kinetics

[a] Units of 10^{13} molecule cm^{-3}. [b] units of 10^{-12} cm^3 molecule^{-1}s^{-1}; statistical 2σ uncertainty is given, total estimated uncertainty is 15%. [c] HW: halocarbon wax; Q: quartz. [d] k_1 derived from H_2S (H_2S kinetics) or H-atom (H kinetics) decays monitored in excess of H and H_2S, respectively.

Examples of H_2S decays observed at different excess concentrations of hydrogen atoms are shown in Figure 1. The consumption of the excess reactant, H atoms, along the reaction zone did not exceed a few percent (mainly due to the wall loss, k_w < 10 s^{-1}). In all cases, the average concentration of H was used in the calculations. The concentration of H_2S decays exponentially, $[H_2S] = [H_2S]_0 \times \exp(-k_1' \times t)$, where $k_1' = k_1[H]$ is the pseudo-first-order rate constant of H_2S loss.

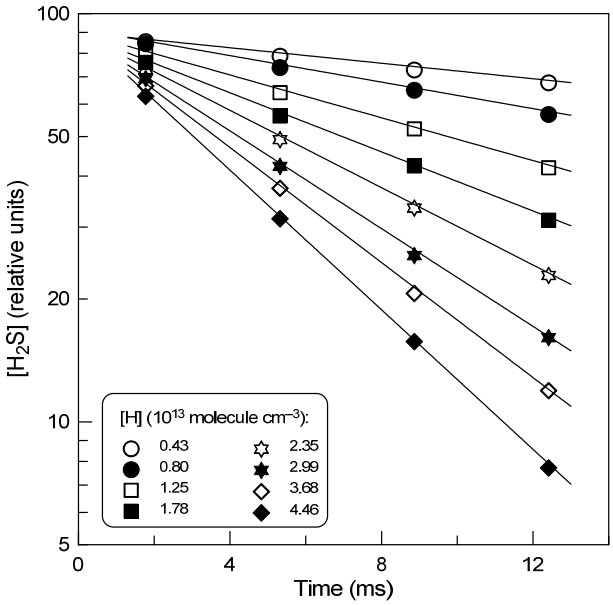

Figure 1. Reaction H + H_2S: example of H_2S decays observed with different concentrations of H atoms at T = 575 K.

The pseudo-first-order rate constants, k_1', determined from the slopes of the straight lines like those in Figure 1, are shown in Figure 2, as a function of H-atom concentration.

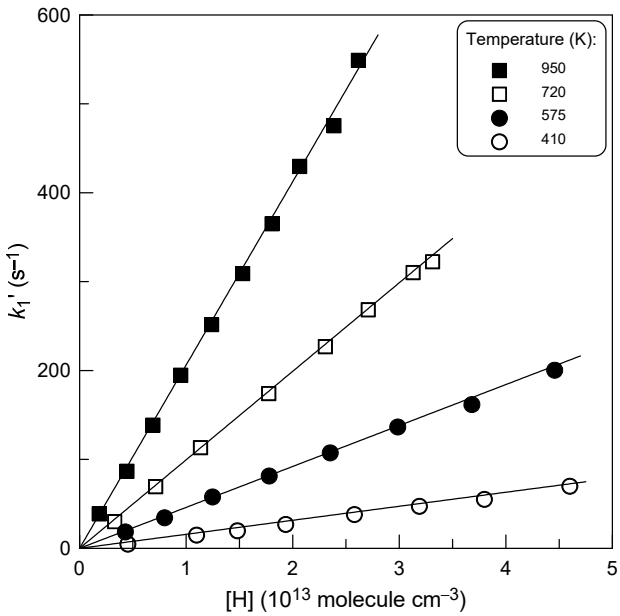

Figure 2. Reaction H + H_2S: dependence of the pseudo-first-order rate constant, $k_1' = k_1[H]$, on the concentration of H atoms at different temperatures.

One can note that the intercepts in Figure 2 are close to zero, which is consistent with the observed lack of H_2S consumption in the absence of hydrogen atoms in the reactor. Diffusion corrections were applied to all the measured values of k_1' in order to take into account the axial and radial gradient of H_2S concentration in the flow tube [25]. Corrections were generally less than 3%, and only at T = 950 K were they somewhat higher, reaching 7%. The slopes of the straight lines in Figure 2 provide the bimolecular rate constants at respective temperatures, which are summarized in Table 1.

In the second series of experiments, the kinetics of H-atom consumption in an excess of hydrogen sulfide was recorded. Figure 3 displays typical exponential decays of [H] with

time, $[H] = [H]_0 \times \exp(-k_1' \times t)$, where $k_1' = k_1[H_2S] + k_w$ is the pseudo-first-order rate constant, with k_w representing the heterogeneous loss of H atoms.

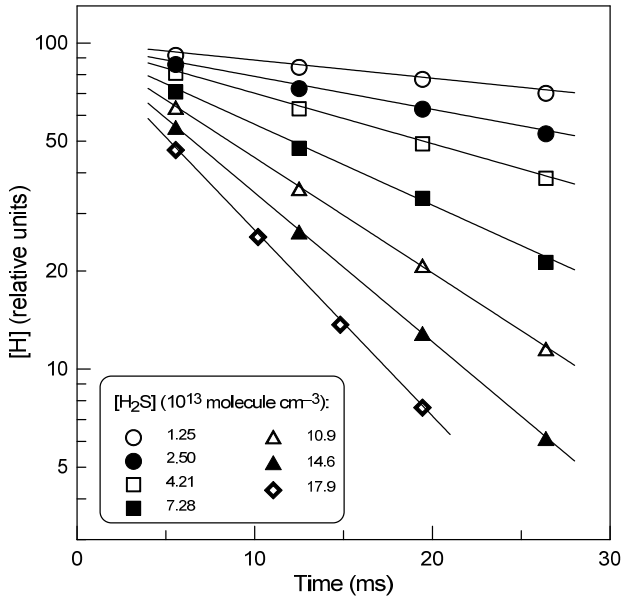

Figure 3. Reaction H + H_2S: typical H-atom decays observed in the presence of different concentrations of H_2S at T = 325 K.

Examples of the typical second-order plots observed at different temperatures are shown in Figure 4. The low intercept values of the plots in Figure 4 are in agreement with the wall loss rate of H atoms, $k_w < 10\ s^{-1}$, measured in the absence of H_2S in the reactor. Diffusion corrections applied to the measured values of k_1' did not exceed 10%. Final values of k_1 determined in this series of experiments are presented in Table 1. The combined uncertainty on k_1 was estimated to be around 15% for both series of experiments by adding in quadrature statistical error (≤2%) and those on the measurements of the absolute concentration of H_2S (≈7%), (H) (≈10%), flows (3%), pressure (2%), and temperature (1%).

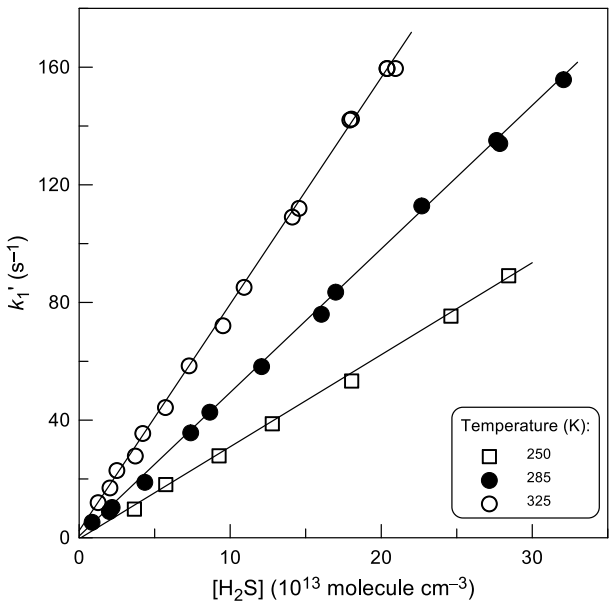

Figure 4. Reaction H + H_2S: dependence of the pseudo-first order rate constant, $k_1' = k_1[H_2S] + k_w$, on the concentration of H_2S at different temperatures.

Reaction (1) produces SH radicals, and H-atom kinetics can be potentially impacted by the fast secondary reaction:

$$H + SH \rightarrow S + H_2 \quad (3)$$

The rate constant of reaction (3) is not well known. Measurements of k_3 available in the literature are scattered between 1.1×10^{-11} and 4.15×10^{-11} cm^3 molecule^{-1} s^{-1} at room temperature [4,8,10,26]. Although this secondary reaction is quite fast, its impact on the measurements of k_1 can be considered negligible due to the low initial concentrations of H atoms used ($[H]_0 \leq 2 \times 10^{11}$ molecule cm^{-3}).

2.1.2. Comparison with Previous Data

Figure 5 shows the temperature-dependent data available for k_1. As noted in the Introduction section and as can be seen in Figure 5, the rate constant for reaction (1) is relatively well established.

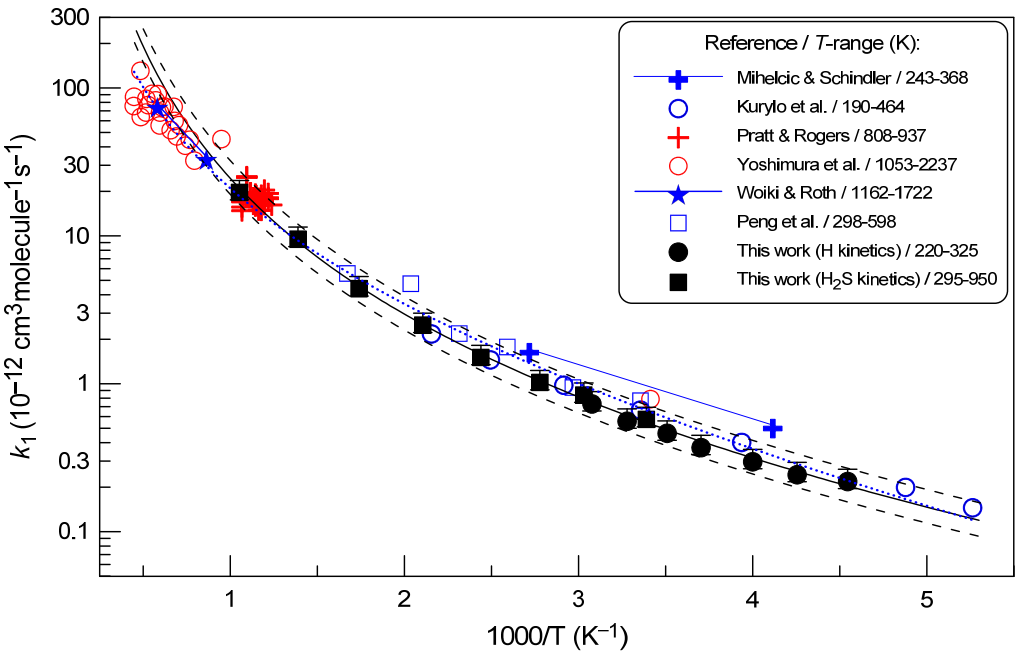

Figure 5. Temperature dependence of the rate constant of reaction (1). Uncertainties shown for the present measurements of k_1 correspond to estimated total uncertainty of 15%.

The most reliable measurements of k_1 at room temperature [8,10–12] (not shown in Figure 5 for clarity) are in good agreement with each other. Bradley et al. [8] measured k_1 in a flow reactor using electron spin resonance for detection of hydrogen atoms: $k_1 = 8.3 \times 10^{-13}$ cm^3 molecule^{-1} s^{-1}. The same value was reported for k_1 by Nicholas et al. [10] who monitored the concentrations of SH and S_2 intermediates upon decomposition of H_2S in a pulsed radio-frequency discharge and derived k_1 from computer simulation of SH and S_2 profiles. Husain and Slater [11] reported an absolute value of $k_1 = (8.6 \pm 0.5) \times 10^{-13}$ cm^3 molecule^{-1} s^{-1}, determined via the pulsed photolysis resonance fluorescence method. Finally, Clyne and Ono [12] measured $k_1 = (7.41 \pm 0.39) \times 10^{-13}$ cm^3 molecule^{-1} s^{-1}, employing resonance fluorescence method in a discharge flow system. It can be noted that the present value of k_1 measured around room temperature, e.g., $(6.0 \pm 0.9) \times 10^{-13}$ cm^3 molecule^{-1} s^{-1} at T = 295 K, is somewhat lower than these previous measurements.

The first temperature-dependent measurement of the rate constant for reaction (1) was conducted by Mihelcic and Schindler [5], who used a discharge flow system combined with ESR detection of hydrogen atoms. The following Arrhenius equation was reported: $k_1 = (1.7 \pm 0.1) \times 10^{-11} \exp(-845 \pm 25)/T]$ cm^3 molecule^{-1} s^{-1} at T = 243–368 K. Kurylo et al. [6], using flash photolysis coupled with resonance fluorescence, carried out absolute

measurements of k_1 over a temperature range of 190–464 K, and reported k_1 = (1.29 ± 0.15) × 10^{-11} exp[−(860 ± 30)/T] cm^3 $molecule^{-1}$ s^{-1}. At high temperatures (T > 800 K), the rate constant of reaction (1) has been determined in three studies [9,13,14]. Pratt and Rogers [9] in their mass spectrometric study of the early stages of the exchange reaction in H_2S/D_2 mixture deduced values of k_1 at T = 808–937 K, which are shown in Figure 5. Yoshimura et al. [13] and Woiki and Roth [14] studied reaction (1) behind reflected shock waves, applying atomic resonance absorption spectroscopy for the measurements of H-atom concentration, and reported k_1 = 3.2 × 10^{-10} exp(−2491/T) at T = 1053–2237 K and k_1 = 4.15 × 10^{-10} exp(−2890/T) cm^3 $molecule^{-1}$ s^{-1} at T = 1160–1722 K, respectively. As one can see in Figure 5, the results of these high temperature measurements are in good agreement. Finally, in the most recent study of the reaction (1) [15], k_1 was measured via the flash photolysis resonance fluorescence technique and found to be: k_1 = 6.6 × 10^{-11} exp(−1347/T) cm^3 $molecule^{-1}$ s^{-1} at T = 298–598 K.

The present measurements of k_1 are in very good agreement with those of Kurylo et al. [6], Pratt and Rogers [9], and, in the range of experimental uncertainty, with the data from Peng et al. [15]. The k_1 values measured by Mihelcic and Schindler [5] are a bit higher than others. Rommel and Schiff [7] suggested that the k_1 values reported by Michelcic and Schindler [5] may have been overestimated. In fact, the values of k_1 were derived from decays of H atoms under experimental conditions, where initial H_2S concentration was comparable to that of hydrogen atoms. In addition, secondary reaction (3), which should operate under such conditions, was not taken into account.

The present data for k_1 obtained in a wide temperature range clearly show a well-pronounced curvature of the Arrhenius plot. The fit of the current data with the modified Arrhenius expression (the continuous black line in Figure 5) yields

$$k_1 = 8.7 \times 10^{-13} \times (T/298)^{2.87} \times \exp(-125/T)\ cm^3\ molecule^{-1}\ s^{-1}.$$

This expression for k_1 is recommended from the present study in the temperature range 220–950 K, with a conservative (independent of temperature) overall 2σ uncertainty of 15%. The black dashed lines in Figure 5 represent the deviations from this equation by a factor of 1.3, showing that practically all existing data (except at the highest temperatures) fall into this range.

It should be noted that the curvature of the Arrhenius plot is observed experimentally for the first time, although it was suggested in some previous studies. All previous experimental work was carried out over a limited temperature range, and resulted in "unmodified" Arrhenius expressions for k_1. Yoshimura et al. [13] based on their measurements of k_1 at room and high temperatures (Figure 5) suggested a strong non-Arrhenius dependence of k_1 on temperature, which was explained by a conventional transition-state theory combined with ab initio calculations. Peng et al. [15], combining their experimental data (T = 298–598 K) with those available in the literature, reported k_1 = 5.8 × 10^{-17} × $T^{1.94}$ exp(−455/T) cm^3 $molecule^{-1}$ s^{-1} (blue dotted line in Figure 5). This expression reasonably (within 25%) describes the k_1 data from the present work. The theoretical analysis carried out by the authors also supported the significant curvature of the Arrhenius plot. The experimentally observed non-Arrhenius temperature dependence of k_1 was also reasonably reproduced by the recent quantum dynamics calculations of Qi et al. [2], concluding that the non-Arrhenius behavior is caused by the pronounced quantum tunneling. The calculations of Qi et al. [2] showed that both abstraction and exchange mechanisms are important for the H + H_2S reaction. Unfortunately, the available experimental data do not make it possible to define the contribution of these two mechanisms as a function of temperature.

2.2. Reaction H + C_2H_4S

2.2.1. Measurements of the Reaction Rate Constant

A similar experimental protocol described above for reaction (1) was also applied to measure the rate constant of the reaction of hydrogen atoms with thiirane. As in the previous case, the rate constant of reaction (2) was determined under pseudo-first order

conditions by two methods: from kinetics of thiirane consumption ($[C_2H_4S]_0 \leq 3.6 \times 10^{11}$ molecule cm^{-3}) in excess of hydrogen atoms and from H-atom decays ($[H]_0 \leq 2.1 \times 10^{11}$ molecule cm^{-3}) recorded in excess of C_2H_4S. The concentrations of the corresponding excess reactants are shown in Table 2. The flow velocity in the reactor was in the range (1045–3250) cm s^{-1}. Examples of second-order plots obtained from C_2H_4S and H-atom decays are shown in Figures 6 and 7, respectively. The similarity of the results obtained with different initial concentrations of C_2H_4S (Figure 6, T = 220 K) and hydrogen atoms (Figure 7) indicates a minor influence of possible secondary chemistry on the measurements of k_2. The final values of k_2 determined at different temperatures from the slopes of the straight lines like those in Figures 6 and 7 are shown in Table 2.

Table 2. Experimental conditions and results of the measurements of the rate constant of reaction (2).

T (K)	[Excess Reactant] [a]	k_2 [b]	Reactor Surface [c]	Method [d]
220	0.21–9.19	1.67 ± 0.04	HW	C_2H_4S kinetics
225	0.40–8.82	1.77 ± 0.03	HW	C_2H_4S kinetics
235	0.8–7.73	2.05 ± 0.04	HW	C_2H_4S kinetics
245	0.26–7.25	2.11 ± 0.03	HW	C_2H_4S kinetics
250	0.23–3.86	2.26 ± 0.06	HW	H kinetics
255	0.45–8.28	2.35 ± 0.04	HW	C_2H_4S kinetics
270	0.24–4.03	2.56 ± 0.07	HW	H kinetics
270	0.56–6.44	2.7 ± 0.04	HW	C_2H_4S kinetics
275	0.48–6.73	2.75 ± 0.07	HW	C_2H_4S kinetics
297	0.11–3.84	3.54 ± 0.04	Q	C_2H_4S kinetics
320	0.33–6.03	4.36 ± 0.04	HW	C_2H_4S kinetics
325	0.36–4.86	4.35 ± 0.08	HW	H kinetics
330	0.30–4.54	4.99 ± 0.06	HW	C_2H_4S kinetics
360	0.23–3.34	5.71 ± 0.06	Q	C_2H_4S kinetics
410	0.18–2.58	8.23 ± 0.07	Q	C_2H_4S kinetics
475	0.15–2.24	12.1 ± 0.1	Q	C_2H_4S kinetics
575	0.18–1.94	17.7 ± 0.1	Q	C_2H_4S kinetics
720	0.14–1.36	30.5 ± 0.2	Q	C_2H_4S kinetics
950	0.09–1.08	44.9 ± 0.1	Q	C_2H_4S kinetics

[a] Units of 10^{13} molecule cm^{-3}. [b] units of 10^{-12} cm^3 molecule^{-1}s^{-1}; statistical 2σ uncertainty is given; total estimated uncertainty is 15%. [c] HW: halocarbon wax; Q: quartz. [d] k_2 derived from C_2H_4S (C_2H_4S kinetics) or H-atom (H kinetics) decay monitored in excess of H and C_2H_4S, respectively.

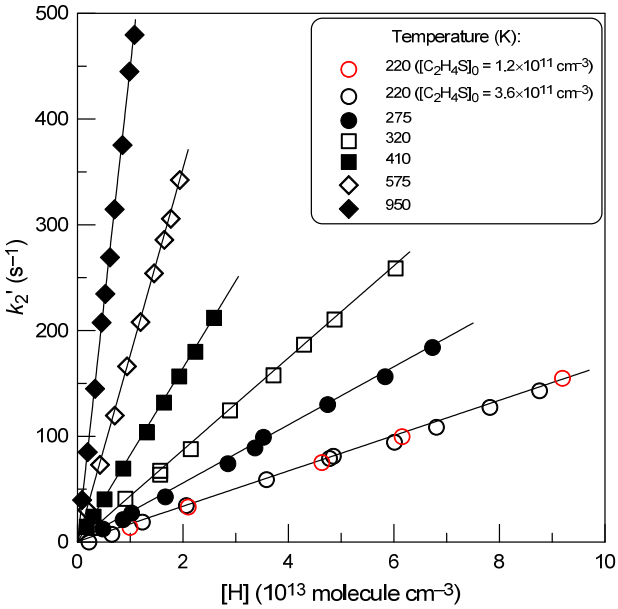

Figure 6. Reaction H + C_2H_4S: pseudo-first-order rate constant, $k_2' = k_2[H]$, as a function of the concentration of H atoms at different temperatures.

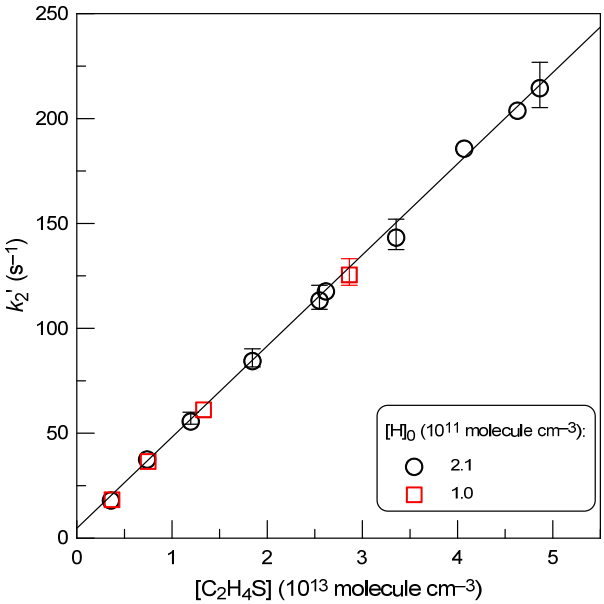

Figure 7. Reaction H + C_2H_4S: dependence of the pseudo-first-order rate constant, $k_2' = k_2[C_2H_4S] + k_w$, on the concentration of C_2H_4S at T = 325 K measured with two different initial concentrations of H atoms.

2.2.2. Comparison with Previous Data

The rate constant of the H + C_2H_4S reaction is displayed as a function of temperature in Figure 8. The present data on the temperature dependence of k_2 are best represented by the sum of two exponential functions (the continuous black line in Figure 8):

$$k_2 = 1.85\times10^{-10}\exp(-1410/T) + 4.17\times10^{-12}\exp(-242/T)\ \text{cm}^3\ \text{molecule}^{-1}\ \text{s}^{-1}$$

at T = 220–950 K (with an estimated conservative uncertainty of 15% at all temperatures).

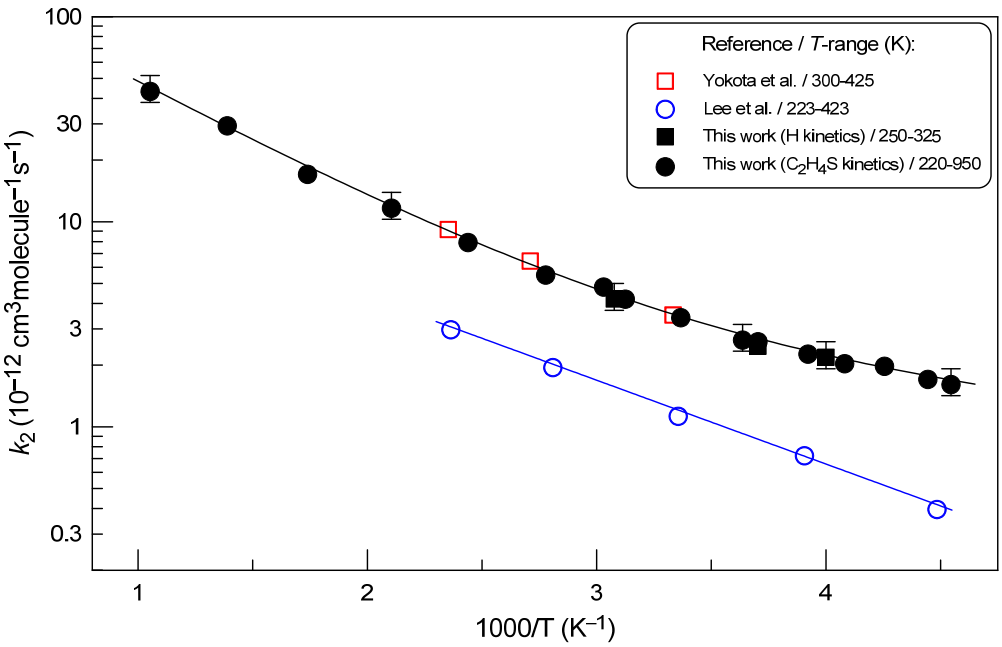

Figure 8. Summary of the measurements of k_2. Uncertainties shown for selected present measurements of k_2 correspond to the estimated total uncertainty of 15%.

To our knowledge, only two studies of the reaction are available in the literature. Yokota et al. [24] studied the reaction of thiirane with hydrogen atoms produced from the mercury photosensitization of H_2. The reaction rate constant was determined relative to that of the H-atom reaction with H_2S at three temperatures between 300 and 425 K: $k_2 = (9.5 \pm 1.2) \times 10^{-11} \exp[-(980 \pm 88)/T]$ cm^3 molecule^{-1} s^{-1}. The relative rate data were placed on an absolute basis with the values of k_1 reported by Kurylo et al. [6], which can be considered valid to date (see Figure 5). Lee et al. [20] carried out absolute measurements of k_2 using the flash photolysis–resonance fluorescence technique, and reported $k_2 = (2.87 \pm 0.12) \times 10^{-11} \exp[-(945 \pm 12)/T]$ cm^3 molecule^{-1} s^{-1} over a temperature range from 223 to 423 K. The present data for k_2 clearly support the results of the relative rate measurements of Yokota et al. [24], being higher by a factor of 3–4 compared with the absolute measurements of Lee et al. [20] (Figure 8). The reason for such a large discrepancy is difficult to determine at this stage. Perhaps the point is in determining the absolute concentrations of thiirane, which (i) was photolyzed in the study of Lee at al. [20] to generate H atoms, and (ii) is known to decompose during storage.

In the study of Yokota et al. [24], C_2H_4, H_2S, and elemental sulfur were detected as reaction products in accordance with the formation of SH radical and C_2H_4 in the primary step, followed by the production of H_2S and S in the self-reaction of SH radicals:

$$SH + SH \rightarrow S + H_2S \tag{4}$$

$$S + C_4H_4S \rightarrow S_2 + C_2H_4 \tag{5}$$

In this work, we also observed the formation of SH, S and S_2 under specific conditions (high concentrations of both reactants); however, quantitative measurements were quite difficult, and were not performed.

3. Materials and Methods

All experiments were performed in a conventional discharge fast-flow reactor coupled with a modulated molecular beam-sampling quadrupole mass spectrometer for the detection of the gas phase species [23]. Two different flow reactors (45 cm length and 2.4 cm i.d.) available in the laboratory were used. The low-temperature flow reactor, a Pyrex tube coated with halocarbon wax with a jacket for the circulation of thermostatically controlled ethanol (Figure 9), covered a temperature range between 220 and 330 K. The high-temperature flow reactor was employed over a temperature range of 295−950 K and consisted of an electrically heated uncoated Quartz tube with water-cooled attachments.

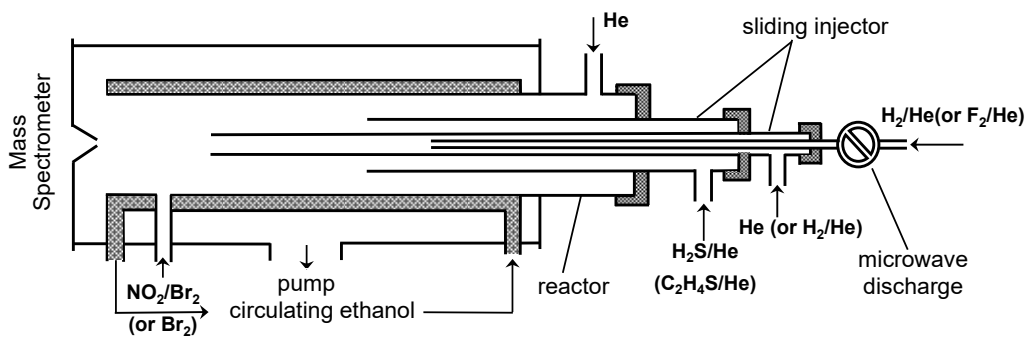

Figure 9. Low-temperature flow reactor: configuration used in the measurements of the rate constants of reactions (1) and (2).

Hydrogen atoms were produced using two methods. The first one employed the microwave discharge of H_2/He mixtures. In the second method, H atoms were formed in the fast reaction of F atoms with H_2,

$$F + H_2 \rightarrow H + HF \tag{6}$$

$k_6 = 1.24 \times 10^{-10} \exp(-507/T)$ cm^3 molecule^{-1} s^{-1} (T = 220–960 K) [27].

In this case, the fluorine atoms were generated in the microwave discharge of F_2/He mixtures and titrated with an excess of H_2 in the movable injector (Figure 9). The fraction of F_2 dissociated in the microwave discharge exceeded 95%. Ensuring that there was no molecular fluorine in the reactor was important in the presence of thiirane, since it was observed that these two stable compounds show high reactivity towards each other.

Low concentrations of hydrogen atoms were monitored using their chemical conversion to stable species HOBr (m/z = 96/98) upon addition of the NO_2/Br_2 mixture 5 cm upstream of the sampling cone of the mass spectrometer (Figure 9). In this configuration, H atoms are converted to HOBr in two successive rapid reactions (7) and (8):

$$H + NO_2 \rightarrow OH + NO \quad (7)$$

$k_7 = (1.47 \pm 0.26) \times 10^{-10}$ cm^3 molecule^{-1} s^{-1} (T = 195–2000 K) [28],

$$OH + Br_2 \rightarrow Br + HOBr \quad (8)$$

$k_8 = 2.16 \times 10^{-11} \exp(207/T)$ cm^3 molecule^{-1} s^{-1} (T = 220–950 K) [29].

The concentrations of NO_2 and Br_2 were chosen so that the hydrogen atoms reacted primarily with NO_2 rather than with Br_2 in reaction (9):

$$H + Br_2 \rightarrow Br + HBr \quad (9)$$

$k_9 = 7.06 \times 10^{-11} (T/298)^{0.88} \exp(182/T)$ cm^3 molecule^{-1} s^{-1} (T = 220–950 K) [30].

In experiments with high concentrations of hydrogen atoms (kinetics of H_2S, and C_2H_4S consumption in excess of H), they were detected at m/z = 80/82 (HBr^+) after being transformed to HBr in reaction (9).

The absolute calibration of the mass spectrometer for HOBr was accomplished using reaction (8) in excess of Br_2, and relating the consumed fraction of Br_2 to the concentration of HOBr produced: [HOBr] = $\Delta[Br_2]$. Absolute HBr concentrations were determined using two methods. In the first method, the absolute concentration of HBr was calculated from the flow rate of a manometrically prepared HBr/He mixture. The second method was the chemical transformation of the H atom into HBr in reaction (9), linking the consumed fraction of Br_2 and the concentration of HBr formed: [HBr] = $\Delta[Br_2]$. The results of the two methods coincided within a few percent. The absolute concentrations of other stable species (Br_2, NO_2, F_2, H_2, H_2S and C_2H_4S) in the reactor were calculated from their flow rates, obtained from the measurements of the pressure drop of their monometrically prepared mixtures in He stored in calibrated volume flasks.

The purities of the gases used were as follows: He > 99.999% (Alphagaz); Br_2 > 99.99% (Aldrich); F_2, 5% in helium (Alphagaz); HBr > 99.8% (Praxair); H_2 > 99.998% (Alphagaz); NO_2 > 99% (Alphagaz); H_2S > 99.5% (Alphagaz); C_2H_4S (Merck), 98%.

4. Conclusions

In this work, we have investigated the kinetics of the reactions of H atoms with hydrogen sulfide and thiirane, using a discharge flow reactor combined with mass spectrometry. For the H + H_2S reaction, previously assumed on the basis of experimental and theoretical data, the strong curvature of the Arrhenius plot was confirmed via measurements of the reaction rate constant over an extended temperature range (220–950 K). Similar curved Arrhenius dependence was also observed for reaction of H atoms with C_2H_4S, which was studied at T = 220–950 K (and for the first time at T > 425 K). The reaction was found to be fast enough to be used as an alternative (free of H_2S) source of SH radicals (an important intermediate in combustion and atmospheric chemistry) in laboratory studies.

Funding: This research was funded by ANR through the PIA (Programme d'Investissement d'Avenir), grant number ANR-10-LABX-100-01.

Institutional Review Board Statement: Not applicable.

Informed Consent Statement: Not applicable.

Data Availability Statement: The data supporting reported results are available in this article.

Conflicts of Interest: The author declares no conflict of interest.

References

1. Sendt, K.; Jazbec, M.; Haynes, B.S. Chemical kinetic modeling of the H/S system: H_2S thermolysis and H_2 sulfidation. *Proc. Combust. Inst.* **2002**, *29*, 2439–2446. [CrossRef]
2. Qi, J.; Lu, D.; Song, H.; Li, J.; Yang, M. Quantum and quasiclassical dynamics of the multi-channel H + H_2S reaction. *J. Chem. Phys.* **2017**, *146*, 124303. [CrossRef]
3. Lamberts, T.; Kästner, J. Tunneling Reaction Kinetics for the Hydrogen Abstraction Reaction H + H_2S → H_2 + HS in the Interstellar Medium. *J. Phys. Chem. A* **2017**, *121*, 9736–9741. [CrossRef]
4. Cupitt, L.T.; Glass, G.P. Reaction of atomic oxygen with hydrogen sulphide. *Trans. Faraday Soc.* **1970**, *66*, 3007–3015. [CrossRef]
5. Mihelcic, D.; Schindler, R.N. ESR-spektroskopische Untersuchung der Reaktion von atomarem Wasserstoff mit H_2S. *Ber. Bunsenges. Phys. Chem.* **1970**, *74*, 1280–1288. [CrossRef]
6. Kurylo, M.J.; Peterson, N.C.; Braun, W. Absolute Rate of the Reaction H+H_2S. *J. Chem. Phys.* **1971**, *54*, 943–946. [CrossRef]
7. Rommel, H.; Schiff, H.I. The Reactions of H Atoms with H_2S and COS. *Int. J. Chem. Kinet.* **1972**, *4*, 547–558. [CrossRef]
8. Bradley, J.N.; Trueman, S.P.; Whytock, D.A.; Zaleski, T.A. Electron spin resonance study of the reaction of hydrogen atoms with hydrogen sulphide. *J. Chem. Soc. Faraday Trans. 1* **1973**, *69*, 416–425. [CrossRef]
9. Pratt, G.; Rogers, D. Homogeneous isotope exchange reactions. Part 3.—H_2S + D_2. *J. Chem. Soc. Faraday Trans. 1 Phys. Chem. Condens. Phases* **1977**, *73*, 54–61. [CrossRef]
10. Nicholas, J.E.; Amodio, C.A.; Baker, M.J. Kinetics and mechanism of the decomposition of H_2S, CH_3SH and $(CH_3)_2S$ in a radio-frequency pulse discharge. *J. Chem. Soc. Faraday Trans. 1 Phys. Chem. Condens. Phases* **1979**, *75*, 1868–1875. [CrossRef]
11. Husain, D.; Slater, N.K.H. Kinetic study of the reactions of hydrogen and deuterium atoms with HBr and DBr by time-resolved resonance fluorescence. *J. Chem. Soc. Faraday Trans. 2 Mol. Chem. Phys. Mol. Chem. Phys.* **1980**, *76*, 276–285. [CrossRef]
12. Clyne, M.A.A.; Ono, Y. Determination of the rate constant of reaction of ground-state CI and H atoms with H_2S using resonance fluorescence in a discharge flow. *Chem. Phys. Lett.* **1983**, *94*, 597–602. [CrossRef]
13. Yoshimura, M.; Koshi, M.; Matsui, H.; Kamiya, K.; Umeyama, H. Non-Arrhenius temperature dependence of the rate constant for the H + H_2S reaction. *Chem. Phys. Lett.* **1992**, *189*, 199–204. [CrossRef]
14. Woiki, D.; Roth, P. A Shock Tube Study of the Reactions of H Atoms with COS, CS_2, and H_2S. *Isr. J. Chem.* **1996**, *36*, 279–283. [CrossRef]
15. Peng, J.; Hu, X.; Marshall, P. Experimental and ab Initio Investigations of the Kinetics of the Reaction of H Atoms with H_2S. *J. Phys. Chem. A* **1999**, *103*, 5307–5311. [CrossRef]
16. Kurosaki, Y.; Takayanagi, T. Theoretical study of the non-Arrhenius temperature dependence of thermal rate constants for the H+H_2S → H_2+SH reaction. *J. Chem. Phys.* **1999**, *111*, 10529–10536. [CrossRef]
17. Bedjanian, Y. Rate constant and products of the reaction of $O(^3P)$ atoms with thiirane over the temperature range 220–950 K. *Int. J. Chem. Kinet.* **2022**, *54*, 552–558. [CrossRef]
18. Murrells, T.P. Elementary reactions of the SCl radical. Part1.—Rate constants and mechanisms of the reaction Cl + C_2H_4S → SCl + C_2H_4, SCl + SCl → products and SCl + Cl_2 → SCl_2+ Cl. *J. Chem. Soc. Faraday Trans. 2 Mol. Chem. Phys.* **1988**, *84*, 67–83. [CrossRef]
19. Van Roodselaar, A.; Safarik, I.; Strausz, O.P. The reactions of $S(^3P_J)$ atoms with thiiranes. *Int. J. Chem. Kinet.* **1984**, *16*, 899–907. [CrossRef]
20. Lee, J.H.; Stief, L.J.; Timmons, R.B. Absolute rate parameters for the reaction of atomic hydrogen with carbonyl sulfide and ethylene episulfide. *J. Chem. Phys.* **1977**, *67*, 1705–1709. [CrossRef]
21. Hynes, A.J.; Wine, P.H. Kinetics and Mechanisms of the Oxidation of Gaseous Sulfur Compounds. In *Gas-Phase Combustion Chemistry*; Gardiner, W.C., Ed.; Springer: New York, NY, USA, 2000; pp. 343–388.
22. Tyndall, G.S.; Ravishankara, A.R. Atmospheric oxidation of reduced sulfur species. *Int. J. Chem. Kinet.* **1991**, *23*, 483–527. [CrossRef]
23. Bedjanian, Y. Rate Coefficients of the Reactions of Fluorine Atoms with H_2S and SH over the Temperature Range 220–960 K. *Molecules* **2022**, *27*, 8365. [CrossRef]
24. Yokota, T.; Ahmed, M.G.; Safarik, I.; Strausz, O.P.; Gunning, H.E. Reaction of hydrogen atoms with thiirane. *J. Phys. Chem.* **1975**, *79*, 1758–1762. [CrossRef]
25. Kaufman, F. Kinetics of elementary radical reactions in the gas phase. *J. Phys. Chem.* **1984**, *88*, 4909–4917. [CrossRef]
26. Langford, R.B.; Oldershaw, G.A. Flash photolysis of H_2S. *J. Chem. Soc. Faraday Trans. 1 Phys. Chem. Condens. Phases* **1972**, *68*, 1550–1558. [CrossRef]
27. Bedjanian, Y. Rate constants for the reactions of F atoms with H_2 and D_2 over the temperature range 220-960 K. *Int. J. Chem. Kinet.* **2021**, *53*, 527–535. [CrossRef]

28. Su, M.C.; Kumaran, S.S.; Lim, K.P.; Michael, J.V.; Wagner, A.F.; Harding, L.B.; Fang, D.C. Rate Constants, $1100 \leq T \leq 2000$ K, for H + NO_2 → OH + NO Using Two Shock Tube Techniques: Comparison of Theory to Experiment. *J. Phys. Chem. A* **2002**, *106*, 8261–8270. [CrossRef]
29. Bedjanian, Y. Temperature-Dependent Rate Constant for the Reaction of Hydroxyl Radical with 3-Hydroxy-3-methyl-2-butanone. *J. Phys. Chem. A* **2019**, *123*, 10446–10453. [CrossRef]
30. Bedjanian, Y. Rate constant of H atom reaction with Br_2 determined between 220 and 950 K. *Chem. Phys. Lett.* **2023**, *825*, 140616. [CrossRef]

Disclaimer/Publisher's Note: The statements, opinions and data contained in all publications are solely those of the individual author(s) and contributor(s) and not of MDPI and/or the editor(s). MDPI and/or the editor(s) disclaim responsibility for any injury to people or property resulting from any ideas, methods, instructions or products referred to in the content.